Proceedings of the 10th World Congress on Mechanical, Chemical, and Material Engineering (MCM'24)
Barcelona, Spain –August 22-24, 2024
Paper No. HTFF 135
DOI: 10.11159/htff24.135

Pressure Drop and Flow Loss Approximation by Comparison between Mathematical Model and Numerical Model of a Simplified Fluid Mount.

Alfiya Ashraf[1], Nader Vahdati[1], Yap Yit Fatt[1]
[1]Khalifa University, Mechanical and Nuclear Engineering Department,
SAN Campus, Abu Dhabi, UAE 127788
100062575@ku.ac.ae, nader.vahdati@ku.ac.ae, yap.fatt@ku.ac.ae

Abstract – Vibration isolators like hydraulic engine mounts are employed in the automotive industry to mitigate the effect of vibration and noise produced in the vehicle by the engine. Several analyses on the transient response of the hydraulic engine mounts have been carried out in literature to improve the performance of the device. In this paper, efforts have been taken to study the oscillatory fluid flow behaviour of the working fluid inside these mounts. A simplified fluid mount model is considered, and its respective numerical and mathematical models are developed to study the effect of input parameters such as frequency and displacement on pressure loss across the inertia track. Comparison of the inertia track pressure loss obtained from both the models provides validation on the modelling approach. This approach can be further utilized to develop a correlation between, the input displacement, the inertia track geometry, the fluid density and viscosity and the pressure loss across the inertia track in hydraulic engine mounts and thereby enhancing the damping efficiency of these mounts.

Keywords: Hydraulic engine mounts, fluid mounts, hydraulic dampers, oscillatory fluid flow, computational fluid dynamics.

1. Introduction

A fully articulated main rotor system of a helicopter has three hinges per blade, pitch hinge, flapping hinge, and a lead-lag hinge. The lead-lag hinge allows the blade to move forward and backward in the plane of the rotor disk. Ground resonance is a mechanical instability affecting helicopters on the ground. It occurs at certain rotor speeds, where the lead–lag motion of the rotor blades couples with the motion of the fuselage, creating a self-excited oscillation, which is very violent and generally can result in total destruction of the helicopter, if the pilot is not careful and well trained. To control the ground resonance, passive hydraulic dampers are used in between the consecutive rotor blades of the main and tail rotors, as shown in Figure 1.

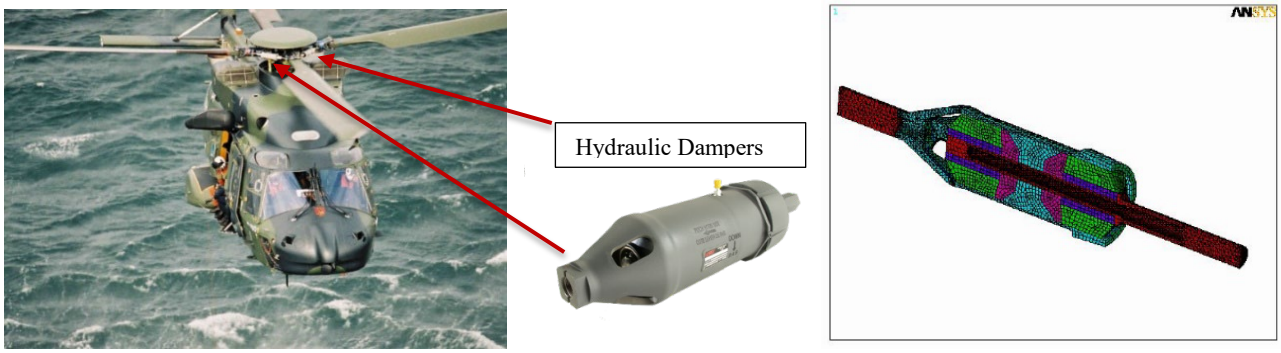

Fig. 1: NH90 helicopter with hydraulic dampers in between the main rotor blades[1]

The internal design, of the hydraulic dampers, is shown in Figure 1 [1]. The hydraulic dampers, used in helicopters, consist of: (1) two fluid chambers (shown in pink color) connected to one another via a carefully designed orifice or inertia track, (2) a carefully selected working fluid (shown in blue color), (3) two rubber tube-forms (shown in green color), (4) a shaft (shown in black color) that connects the two inner members (shown in dark blue color) of the tube-forms, and (5) an outer housing. The carefully selected fluid and designed orifice/inertia track is what makes this damper to work. The damper needs to provide an adequate amount of damping to control the helicopter ground resonance. The lead-lag motion of the

blades makes the working fluid of the hydraulic damper to move back and forth between the two fluid chambers, creating oscillatory fluid flow phenomenon.

There is another passive technology, called hydraulic engine mounts (or fluid or fluidlastic mounts), shown in Figure 2, that also experience oscillatory fluid flow phenomenon. As seen in Figure 2, a passive fluid (or hydraulic) engine mount [2, 3, 4] comprises of a fluid (shown in blue color) that is housed in two elastomeric cavities (or fluid chambers) that are joined by an inertia track.

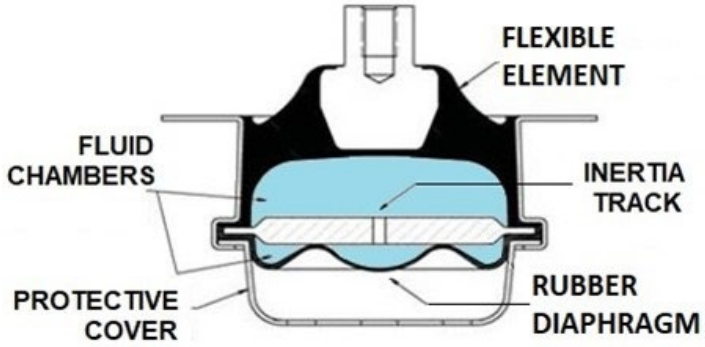

Fig. 2: Hydraulic (fluid) engine mount

The pressure drop from one fluid chamber to the other can be shown as follows:

$$\Delta P = I_f \dot{Q} + \Delta P_L \tag{1}$$

where fluid inertia is equal to $I_f = C\frac{\rho L_t}{A_t}$. In fluid inertia equation, ρ is the working fluid density, L_t is the actual length of the inertia track, CL_t is the effective length of the inertia track with the constant C being in the range of 1 to 4/3 [5], and A_t is the inertia track cross-sectional area. In Equation (1), Q is the flow rate through the inertia track. The 2nd term in the equation (1) includes the effects of viscous shear, expansion/contraction, and other forces such as body and gravitational forces. In this paper, we refer to the 2nd term of equation (1) as the flow losses. Accurate knowledge of the orifice/inertia track flow losses and the effective length of the inertia track are the most important design parameters, when designing a hydraulic damper or a fluid mount. For the hydraulic dampers, since the length of the inertia track is in general low thus low fluid inertia, the 2nd term in the equation (1), namely ΔP_L, is the most important design parameter. For fluid mounts, accurate knowledge of both the effective inertia track length and the flow losses is very much needed. In order to accurately know the constant C and ΔP_L, both CFD and experimental results are needed. Here in this paper, the CFD numerical results are only shown.

Although real fluid mounts and hydraulic dampers can have very complicated geometries, the simplified geometry shown in Figure 3a can be used to characterize the critical device parameters. In the physical model of Figure 3a, the walls of the end chambers are assumed rigid. This allows an isolation of the fluid mechanics effects from the elastomer compliance effects, which can be analysed separately. Here in this paper, we focus on fluid mounts rather than hydraulic dampers since both the inertia track effective length as well as its flow losses will be important.

As we apply a sinusoidal displacement across the chambers of Figure 3a, the fluid is forced to move through the narrow inertia track causing a pressure drop across the mount. To determine the efficiency and improve the performance of the mount, the prediction of this pressure drop is an important criterion. Therefore, the magnitude of the pressure drop, which is a function of inertia track geometry, fluid density and viscosity, and input displacement, is analysed by considering a Physical model which is simulated in MATLAB and ANSYS FLUENT.

2. Numerical Model of the Simplified Fluid Mount Model

The numerical modelling and analysis of the oscillating fluid flow in the simplified fluid mount model is being carried out using CFD tool ANSYS Fluent. The preliminary objective of the approach is to model the oscillating fluid flow in a test section and to initially identify and measure the pressure drop across the inertia track and validate the data with the mathematical model developed.

The problem is solved in a two-dimensional CFD grid. It is initially assumed that there is no heat transfer or heat loss across the walls of the simplified fluid mount model and there is no phase change accounted for during the simulation i.e., the liquid flow is single phase, and the fluid is incompressible.

2.1. Computational Domain and Mesh Generation

The simplified fluid mount model is defined with two fluid chambers and an inertia track between them, see Figure 3a. At the end of the two chambers, inlet 1 and inlet 2 are defined, along with the wall and interior surface body. The fluid is allowed to oscillate inside the domain with the applied frequency and displacement. Since the model is axisymmetric, the geometry is modelled across one side of the axis. In Fluent, the axis of symmetry is the x-axis.

In the ANSYS Meshing module, a computational mesh or grid is created. Using common "sizing" methods, a CFD mesh or grid is built with an elemental size of 0.0005m of the surface body to improve performance quality. Figure 3b represents the geometry of the simplified fluid mount model developed in Fluent and the CFD grid's construction. The grid's good quality was demonstrated by the lack of elements with negative computational mesh areas, orthogonality in the range of 0.87-1, and skewness in the range of 0-0.35.

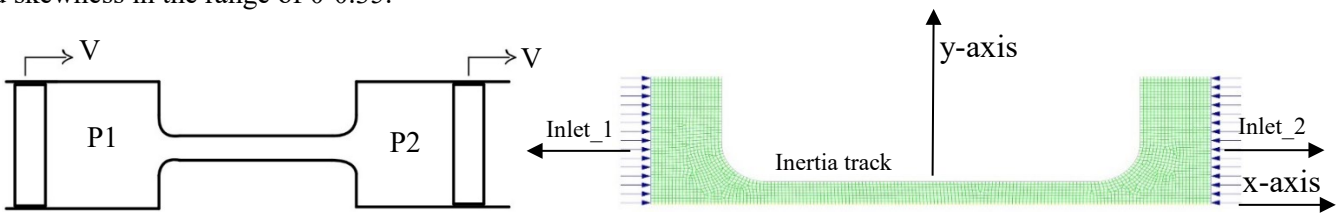

Fig. 3: (a) Physical Model of the Simplified Fluid Mount Model (b) Domain of simulation with inlets and mesh

2.2. Mathematical Description

The oscillating flow inside the flow bench is hydrodynamically fully developed in the inertia track with diameter d_t. The equation is considered by omitting the component of twisting flow, neglecting external forces, the flow direction is assumed to be parallel to the x-axis therefore the velocity has x-direction component only, which also indicated that the velocity to be constant in the direction that is parallel to the centre line. The governing conservation equation for the mass and momentum for the incompressible fully developed flow is expressed as;

$$\frac{\partial u}{\partial x} = 0 \tag{2}$$

$$\frac{\partial u}{\partial t} = -\frac{1}{\rho}\frac{\partial p}{\partial x} + \vartheta\left(\frac{\partial^2 u}{\partial r^2} + \frac{1}{r}\frac{\partial u}{\partial r}\right) \tag{3}$$

Where the x, r, u, p, ρ and ϑ represents the axial and radial coordinates, axial velocity, pressure, density, and kinematic viscosity of the fluid respectively. At the inlet_1 and at inlet_2 the boundary condition is set with a piston motion amplitude as 0.508 mm and at a frequency of 25.84Hz. Therefore, the velocity input at inlet_1 and inlet_2 is expressed as.

$$V_1 = V_2 = 0.08\cos(162.357\mathrm{t}) \tag{4}$$

A transient analysis of the oscillating fluid flow is simulated in the ANSYS Fluent, and the solver is pressure-based. The SST k-omega model is used to solve the problem numerically. In this turbulence model, the k-ε model is used to solve near the wall and k-omega model is used in the free stream region, thereby combining the best features of both models. The model uses a blending function to smoothly transition between the two models based on the distance from the wall, thus allowing the model to accurately predict flows with wide range of turbulence levels and flow conditions.

3. Mathematical Model of the Simplified Fluid Mount Model

The physical model of the simplified fluid mount model was shown Figure 3a. This model is developed as a basis for further mathematical modelling and evaluation of design parameters. Since the concerned system is dealing with multiple energy domains, mechanical and fluid systems, bond graph modelling technique [6] is employed for developing the mathematical model of the simplified fluid mount model of Figure 3a.

In the physical model, shown in Figure 3a, an input velocity is applied to the left and right chamber ends in the same direction. This causes the fluid to be displaced from chamber 1 to the inertia track and further to the chamber 2; respectively. The fluid flow from the chamber 1 to chamber 2 through the inertia track is due to the pressure difference that is caused by this moving chamber ends. As the fluid passes through the inertia track, the fluid undergoes flow losses, due to the friction, viscous shear, and surface roughness, and this is one of the major concerns of oscillating flow simulation.

The bond graph model of the physical model of Figure 3a is shown in Figure 4. The mechanical domain and fluid domain of the simplified fluid mount model is incorporated while developing the bond graph model.

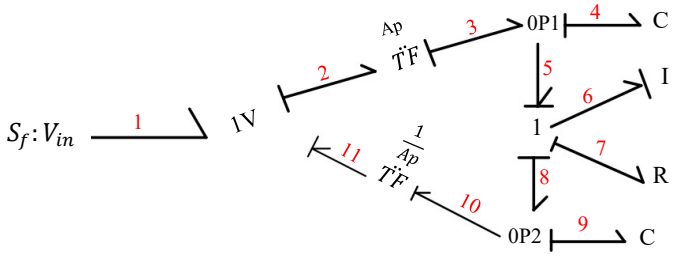

Fig. 4: Bond Graph of the System

In the above bond graph, the input velocity is considered as the source of flow which is represented by bond 1. The mass of the chamber ends can be neglected since we are actuating the ends in a displacement mode. The fluid energy domain is then introduced in the bond graph model when the chamber ends meet the fluid. A transformer is employed for the simplified fluid mount model between the bonds 2 and 3. The employed transformer relation is Q =$A_p V_{in}$, which connects the input velocity to the fluid's volumetric flow rate through the inertia track, which is equal to the chamber end's surface area. Multiple power dissipation factors are encountered as the power flows in the fluid energy domain. Specifically, the fluid's volumetric stiffnesses of each chamber (k_v), inertia track flow losses (R_o), and inertia track fluid inertia (I_f). The compliance represented by C are for the compressibility of the working fluid. The flow losses and fluid inertia inside the inertia track is calculated from the Fluent model. From the bond graph model, the state space equations in terms of displacement and momentum variables are found as shown below,

$$\dot{q}_4 = A_p V_{in} - \frac{P_6}{I_6} \tag{5}$$

$$\dot{P}_6 = \frac{q_4}{C_4} - R_7 \frac{P_6}{I_6} - \frac{q_9}{C_9} \tag{6}$$

$$\dot{q}_9 = \frac{P_6}{I_6} - A_P V_{in} \tag{7}$$

From these state space equations, the state space matrices of the system have been represented below, the output variables are chamber 1 pressure (P_1), and chamber 2 pressure (P_2). MATLAB simulation is carried out with the above represented state space matrices to plot the outputs with respect to time.

$$\begin{bmatrix} q_4 \\ P_6 \\ q_9 \end{bmatrix} = \begin{bmatrix} 0 & -\frac{1}{I_6} & 0 \\ \frac{1}{C_4} & -\frac{R_7}{I_6} & -\frac{1}{C_9} \\ 0 & \frac{1}{I_6} & 0 \end{bmatrix} \begin{bmatrix} q_4 \\ P_6 \\ q_9 \end{bmatrix} + \begin{bmatrix} A_p \\ 0 \\ -A_p \end{bmatrix} V_{in} \tag{8}$$

$$\begin{bmatrix} P_1 \\ P_2 \end{bmatrix} = \begin{bmatrix} \frac{1}{C_4} & 0 & 0 \\ 0 & 0 & \frac{1}{C_9} \end{bmatrix} \begin{bmatrix} q_4 \\ P_6 \\ q_9 \end{bmatrix} + \begin{bmatrix} 0 \\ 0 \end{bmatrix} V_{in} \tag{9}$$

4. Results and Validations

4.1. Numerical Simulation Results

The pressure and velocity contour for the oscillating fluid flow inside the Fluent CFD model is represented in Figures 5 and 6. We can observe that inertia track is said to have a higher value of velocity compared to the chambers. At the same time, considering the total pressure contour, since an input velocity is applied to both sides of the chamber ends which compresses and expands the chambers simultaneously, the total pressure in the chambers is said to have a higher value than the inertia track pressures, which can also be observed from Figure 5. This pressure drop across the chamber results in the motion of fluid through the inertia track. Figure 6 shows the fluid jetting outside of the inertia track, which impacts the inertia track effective.

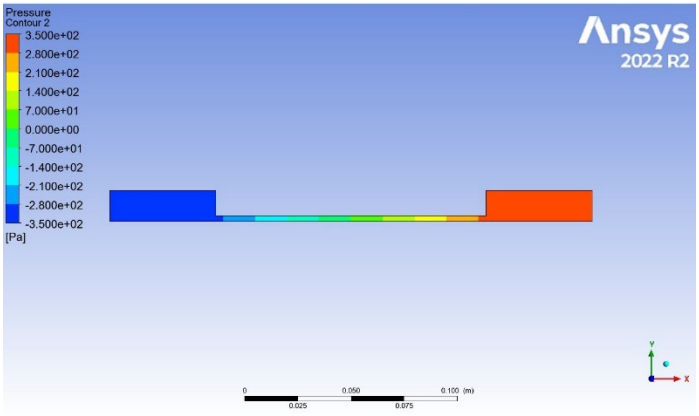

Fig. 5: Pressure contour for flow simulation (fluid flow from right to left)

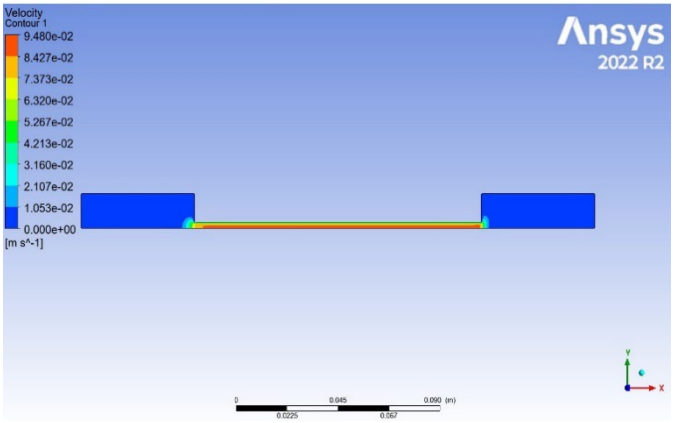

Fig. 6: Velocity contour for flow simulation (fluid flow from right to left)

4.2. Grid Independent Study (Mesh Sensitivity Analysis)

Refinement of mesh is conducted in both spatial and temporal domain. The sinusoidal pressure data is extracted at a point in one of the chambers and the data for the respective refined mesh is represented in the Figure 7. For mesh refinement and comparing the pressure data, we have taken the model parameters as 10 Hz, 0.508 mm, SST K-omega turbulence model, with surface roughness as zero. The working fluid has a density of 1765 Kg/m^3 and 1.8 cst viscosity. From Figure 7, we can conclude that as we refine the mesh in both temporal and spatial domain, the error between each data reduces. Therefore, we can conclude that for the case of 10 Hz, the mesh size of 0.001 and time step size 0.001 can be used for further calculation, as very fine mesh size and time step size may also have large truncation error.

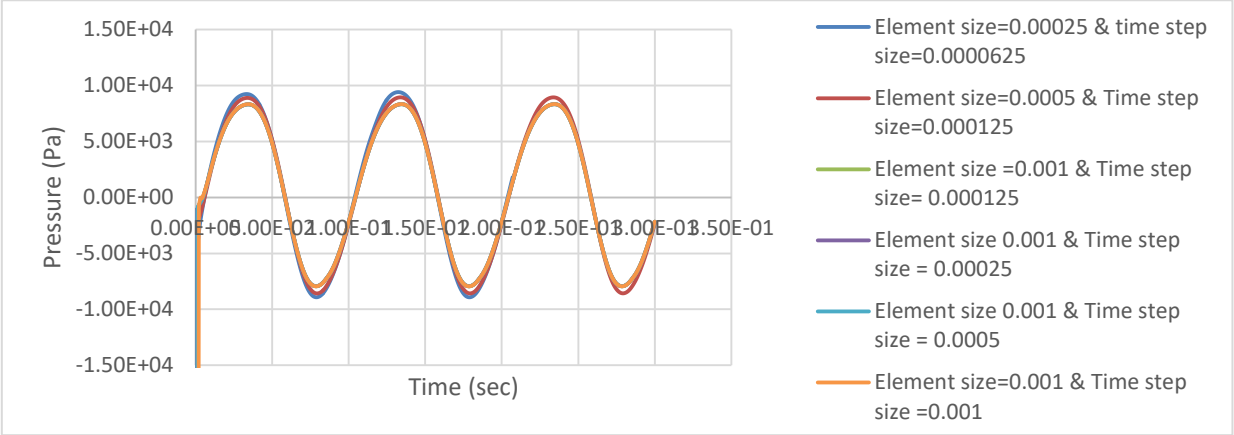

Fig. 7: Pressure data in left chamber at different spatial and temporal refined mesh.

4.3. Parametric Analysis on the Numerical Model

To calculate the pressure drop across the chambers, two points P1 and P2 have been considered shown in Figure 8. The transient pressure data has been extracted at these two points in CFD post processing and the corresponding results of sinusoidal pressure has been plotted in Figure 9. The frequency and displacement for this analysis is taken as 25.84Hz and 0.508mm; respectively. From Figure 9, we can observe that the results have converged as the cycles of pressure is repeating at the same amplitudes. However, we can also observe a shift towards positive y-axis, and this shift could be explained due to the pressure drop accounted by the flow losses. The Table 1 represents the comparison of the pressure data extracted at the points P1 and P2, by changing the numerical model, and surface roughness and by keeping the geometry, boundary conditions and the working fluid the same. From the Table, we can analyse that, the two CFD model SST K-omega and Laminar have a slightly different pressure amplitudes at the two chambers. Also, analysis, on 2D and 3D model has also been done. From comparison of pressure data for 2D versus 3D, we can infer that, the pressure data doesn't have significant difference in its values thus no need to make 3D CFD runs. To see the effect of surface roughness of the chambers and the inertia track on the pressure data, a Fluent simulation was conducted. We can conclude that, as the surface roughness increases the pressure amplitude in two chambers increases there by increasing the pressure drop inside the system. Analysis on the pressure drop with respect to input frequency and displacement has been carried out with another working fluid with the density of 935kg/m^3 and the viscosity of 10 cst.

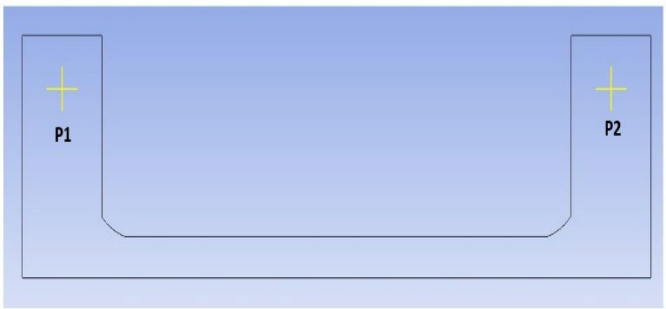

Fig. 8: Location of two points P1 & P2 considered in two chambers.

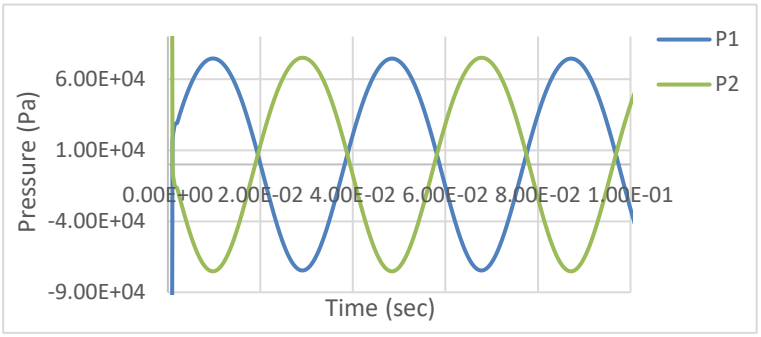

Fig. 9: Pressure data at the points P1 and P2

Table 1: Comparison of pressure data at different CFD model parameters

2D VS 3D	CFD Model	Surface Roughness (m)	Pressure amplitude left chamber, P1 (Pa)	Pressure amplitude right chamber, P2 (Pa)	Reynolds number $Re = \frac{\rho u_{max} d}{\mu}$	Strouhal Number $St = \frac{\omega d}{u_{max}}$
2D	SST k-omega	0	74400	74900	999	44
3D	SST k-omega	0	75900	75800	999	44
2D	Laminar	0	74300	74800	999	44
2D	SST k-omega	0.0005	74700	75300	999	44

From Table 2, we can conclude that as the frequency increases, the pressure drop across the chambers also increases, which represents the square dependence of pressure drop with frequency. If we assume a linear relationship between the pressure drop, ΔP, and the flow rate, Q, and the rate of flow rate, $\dot{Q}$, as shown in equation (10):

$$\Delta P = I_f \dot{Q} + R_o Q \tag{10}$$

where I_f, and R_o represents inertia track fluid inertia, and the flow losses; respectively, then I_f and R_o can be estimated, as shown in Table 2. Similarly, to analyse the influence of displacement amplitude on chamber pressures, numerical simulations have been conducted by keeping all the model and geometry parameters the same as that of the above case, with displacement amplitudes changing from ±0.0381 mm to ±0.0762mm and to ±0.1524mm. The Figure 10 represents the comparison of pressure amplitude at different frequency for the three different displacements amplitudes. Figure 10 shows that the chamber pressures are related to square of the input displacement.

Table 2: Data at constant amplitude and varying frequency

Displacement Amplitude (mm)	Frequency (Hz)	Pressure drop (Pa)	Fluid Inertia $I_f = C\frac{\rho L_t}{A_t}$	Approx Flow Loss, R_0
±0.0381	10	635.6	5927900	1.90E+08
±0.0381	20	2416.1	5937100	2.30E+08
±0.0381	30	5375.3	5950900	2.95E+08
±0.0381	40	9529.8	5997000	3.45E+08
±0.0381	50	14873.5	6020100	4.00E+08
±0.0381	60	21503.9883	6043200	4.88E+08
±0.0381	70	29364.9121	6052400	5.82E+08
±0.0381	80	38310.4082	6089300	6.23E+08
±0.0381	90	48977.3047	6135400	7.04E+08
±0.0381	100	61107.4356	6158500	8.72E+08

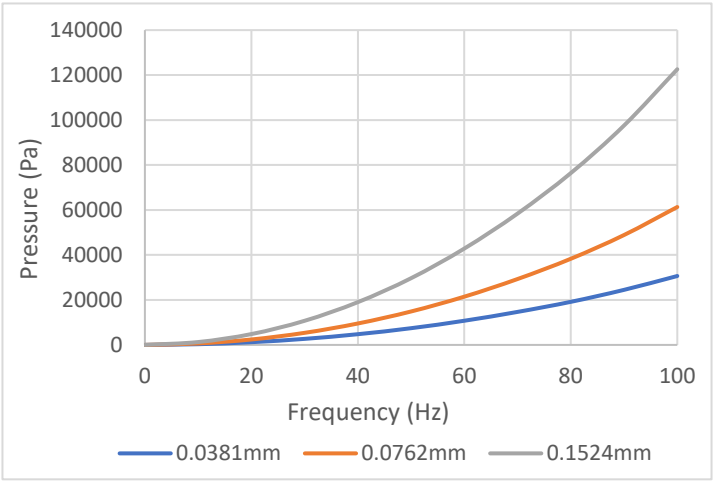

Fig. 10: Pressure amplitude at different displacements

Since in fluid mounts, the location of the notch frequency [2, 3, 4] is directly related to the inertia track fluid inertia and fluid inertia is directly related to the effective length, it is vital to accurately know the effective length of the intertia track through CFD simulations and experimental data. As mentioned in literature, the effective length is equal to 1 to 1.33 times the geometric length [5]. The increase in the effective length could be due to the jetting effect of the fluid from the intertia track at high displacement amplitudes and frequencies. The velocity streamlines shown in Figures 11 and 12 for the case of ±0.0381mm at frequencies of 10 and 100 Hz; respectively, validates the jetting effect theory. This shows the importance of flow visualization.

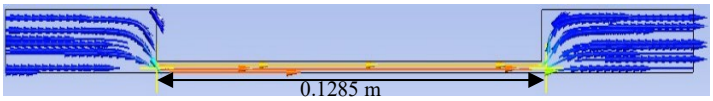

Fig. 11: Effective length of the inertia track for ±0.0381mm @10Hz

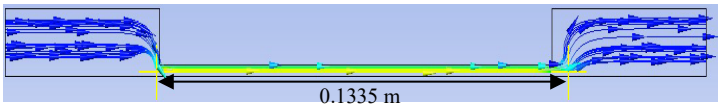

Fig. 12: Effective length of the inertia track for ±0.0381mm @100Hz

4.4. MATLAB Simulation Results

The pressure data obtained from MATLAB simulation is represented in Figure 13. CFD flow visualization, plus the bond graph model is used to find a value for I_f and R_o. The pressure drop for the cases of ±0.0381mm from 10Hz to 100Hz, of CFD model and Mathematical Model, are tabulated below for comparing the accuracy of the pressure data and the effectiveness of the bond graph model to estimate $I_f$and R_o. From the Table 3, we can infer that the pressure drop value obtained from CFD Model and Mathematical model is approximately equal with a maximum error of 3.3%. This increase in percentage error at higher frequencies could be due to the effective length not accurately approximated from the Fluent model.

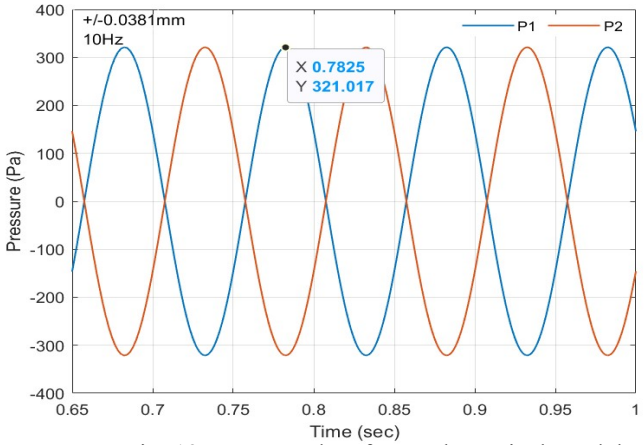

Fig. 13: Pressure data for Mathematical Model

Table 3: Pressure drop comparison for CFD Model and Math Model

Frequency (Hz)	Pressure drop (Pa) **CFD Model**	Pressure drop (Pa) **Mathematical Model**	Percentage error %
10	635.546295	642.034	1.01
20	2416.05396	2406.36	0.4
30	5375.32178	5377.06	0.03
40	9529.78955	9502.46	0.28
50	14873.54052	14978.98	0.7
60	21503.9883	21795	1.33
70	29364.9121	29709.2	1.15
80	38310.4082	39226.2	2.33
90	48977.3047	50412.2	2.84
100	61107.4356	63198.8	3.3

Conclusion

Flow visualization from the CFD Model has clearly indicated the importance of it when determining the effective length of the inertia track used to calculate the fluid inertance, I_f. This provides insights on the importance of using CFD models to develop a relation between the input displacement amplitude and frequency with the effective length of the inertia track, as this length if not calculated correctly, can result in large errors in calculation of the flow losses. The exact values of fluid inertia and flow loss is very important for calculating the exact location and depth of the notch frequency for fluid mounts. Further validation of the CFD and Math models should be carried out using experimental results.

References

[1] D. P. McGuire, “Hybrid Fluid and Elastomer Damper,” U.S. Patent 5 501 434, May 26, 1996.
[2] W. C. Flower, “Understanding hydraulic mounts for improved vehicle noise, vibration and ride qualities,” *SAE Trans.*, pp. 832–841, 1985.
[3] M. Clark, “Hydraulic engine mount isolation,” SAE Technical Paper, 1985.
[4] N. Vahdati, “Variable volumetric stiffness fluid mount design,” *Shock and Vibration*, Vol. 11, issue 1, p. 21, 2004.
[5] E.O. Doebelin, System Dynamics: Modeling Analysis, Simulation, Design, Marcel Dekker, New York, p. 243-244, 1998.
[6] R.C. Rosenberg, D.C. Karnopp, Introduction to Physical Systems Dynamics, Mc Graw Hill Book Company, New York, 1983.